

Hydrophobic Protein–Ligand Interactions Preserved in the Gas Phase

Lan Liu,[†] Dhanashri Bagal,[‡] Elena N. Kitova,[†] Paul D. Schnier,[‡] and John S. Klassen^{*†}

Department of Chemistry, University of Alberta, Edmonton, Alberta, Canada T6G 2G2, and Molecular Structure, Amgen, Thousand Oaks, California 91320

Received July 20, 2009; E-mail: john.klassen@ualberta.ca

The study of the structure and stability of gas-phase noncovalent protein–ligand complexes represents a promising strategy to probe the intrinsic properties of these complexes. Ultimately, new insights about the role of solvent in ligand recognition may be gained from a comparison of protein complexes in the absence and presence of solvent. To date, gas phase studies have focused primarily on protein–ligand complexes stabilized by ionic interactions or hydrogen (H) bonds in solution.¹ These studies have yielded compelling evidence that aspects of solution structure are preserved upon the transfer of protein complexes from solution to the gas phase.¹ For example, a recent electrospray ionization mass spectrometry (ES–MS) study of the structure and stability of protonated and deprotonated gaseous ions of a single chain antibody–trisaccharide complex revealed that several specific intermolecular H-bonds were preserved after desolvation.^{1c} Furthermore, the strength of the H-bonds measured in the gas phase were in good agreement with theoretical values available for model systems.^{1c} As of yet, no detailed gas phase studies of the structure and stability of protein–hydrophobic ligand complexes have been reported, and it is unclear to what extent the nonpolar intermolecular interactions can be probed *in vacuo*. Here, we report evidence from thermal dissociation kinetic measurements and molecular modeling for the preservation of the nonpolar interactions within a series of protein–fatty acid complexes in the gas phase.

Bovine β -lactoglobulin (Lg), an 18 kDa soluble protein, and its interaction with fatty acids (FA), $\text{CH}_3(\text{CH}_2)_x\text{COOH}$, where $x = 10$ (lauric acid \equiv LA), 12 (myristic acid \equiv MA), 14 (palmitic acid \equiv PA), 16 (stearic acid \equiv SA), served as a model system for the present study. At 25 °C, Lg exists predominantly as a homodimer at physiological pH and as monomer at pH >8.² Lg consists of nine β strands (designated A–I), of which the A to H strands form an up-and-down β -barrel, and one major α -helix at the C terminus (Figure S1a, Supporting Information).³ The β -barrel encloses a large cavity ($\sim 315 \text{ \AA}^3$) lined with hydrophobic residues which can accommodate fatty acids and a variety of other hydrophobic ligands (Figure S1b).⁴ The loops above the barrel play important roles in ligand binding. The flexible EF loop forms a lid over the entrance of the cavity and restricts ligand access. A pH-induced conformational change, which occurs in the pH range 6–8, opens the lid and allows access to the cavity.^{2,3} Nuclear magnetic resonance (NMR) spectroscopy measurements identified an increase in conformational flexibility in the EF and GH loops above the barrel upon PA binding to Lg.⁵ It has been suggested that the gain in configurational entropy contributes significantly to the promiscuous, high affinity binding displayed by Lg.⁵

Gaseous deprotonated ions of the (Lg + FA) complexes at charge states -5 to -8 are readily detected in ES–MS performed in negative ion mode on aqueous solutions of Lg and FA at pH

8.5 and 25 °C (Figure S2). Temperature-dependent rate constants (k) for the dissociation of the gaseous (Lg + FA)⁷⁻ ions were determined from time-resolved blackbody infrared radiative dissociation (BIRD) measurements,⁶ which were carried out using Fourier-transform ion cyclotron resonance MS. At the reaction temperatures investigated, 25 to 66 °C, BIRD of the (Lg + FA)⁷⁻ ions proceed exclusively by the loss of neutral FA (Figure S3). Shown in Figure 1a are kinetic data, plotted as the natural log of the normalized intensity of the reactant ion versus reaction time, measured for the loss of PA from the (Lg + PA)⁷⁻ ion. Notably, the kinetic plots exhibit nonlinear behavior that can be described by a double exponential decay function. These results suggest that the (Lg+PA)⁷⁻ ion exists in two kinetically distinct structures, designated as the *fast* and *slow* dissociating components, (Lg + FA)_f and (Lg + FA)_s, respectively. Ion mobility measurements confirmed the presence of two structures for the (Lg+PA)⁷⁻ ion; a single structure was observed for the Lg⁷⁻ ion (Figure S4). The kinetic data measured for the other FAs are also consistent with the presence of two noninterconverting structures (Figure S5). The temperature-dependent k values determined for the *fast* and *slow* components for each FA are shown in the form of Arrhenius plots in Figures 1b and S6. The Arrhenius parameters (E_a and A) and the corresponding entropies of activation (ΔS^\ddagger) are reported in Table 1.

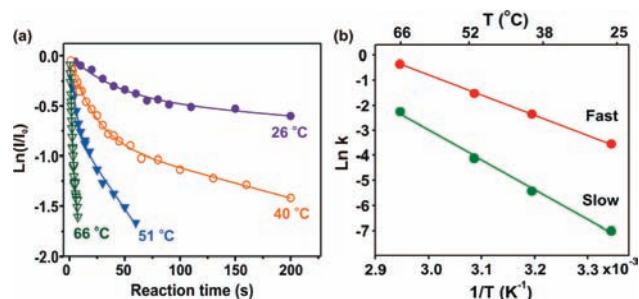


Figure 1. (a) Plots of the natural logarithm of the normalized intensity (I/I_0) of the gaseous (Lg + PA)⁷⁻ ion versus reaction time at the temperatures indicated. The solid curves correspond to the best fit of a double exponential function to the experimental data. (b) Arrhenius plots for the loss of neutral PA from the (Lg + PA)_f⁷⁻ and (Lg + PA)_s⁷⁻ ions.

Inspection of Table 1 reveals that the Arrhenius parameters of both the *fast* and *slow* components are sensitive to the size of the aliphatic chain. However, the parameters of the *fast* components are consistently smaller than those of the *slow* components. The influence of chain length on the dissociation E_a of both components is highlighted in Figure 2a. For the *fast* component, E_a increases almost linearly with chain length, with each methylene group contributing, on average, $0.82 \pm 0.04 \text{ kcal mol}^{-1}$.

This contribution is similar in magnitude to the contribution of individual $-\text{CH}_2-$ groups to the enthalpy changes for the transfer of

[†] University of Alberta.
[‡] Amgen.

Table 1. Arrhenius Parameters (E_a , A) and Corresponding ΔS^\ddagger Values for the Dissociation of the Gaseous $(\text{Lg} + \text{FA})_f^{7-}$ and $(\text{Lg} + \text{FA})_s^{7-}$ Ions^{a,b}

FA	E_a (kcal mol ⁻¹)	A (s ⁻¹)	ΔS^\ddagger (cal mol ⁻¹ K ⁻¹)
		<i>Fast</i>	
LA	13.0 ± 0.7	10 ^{8.4±0.5}	-22 ± 2
MA	14.9 ± 0.4	10 ^{9.5±0.3}	-17 ± 1
PA	16.2 ± 0.3	10 ^{10.2±0.2}	-14 ± 1
SA	18.0 ± 0.6	10 ^{11.3±0.4}	-9 ± 2
		<i>Slow</i>	
LA	25.3 ± 0.9	10 ^{15.4±0.6}	10 ± 3
MA	21.3 ± 1.0	10 ^{13.0±0.7}	-1 ± 3
PA	23.8 ± 0.9	10 ^{14.2±0.6}	5 ± 3
SA	21.5 ± 0.5	10 ^{12.7±0.3}	-2 ± 1

^aThe reported errors are one standard deviation. ^bValues calculated from the corresponding A -factors at 298 K.

n -alkanes from the gas phase to nonpolar solvents, e.g., 1.18 ± 0.02 (n -C₇H₁₆) and 1.04 ± 0.04 (C₆H₆).⁷ Furthermore, the magnitude of the E_a values agree reasonably well with the solvation enthalpies predicted for the aliphatic chains of the FAs in nonpolar and weakly polar solvents (Figure 2b).⁸ Taken together, these results suggest that, in the $(\text{Lg} + \text{FA})_f^{7-}$ ions, the aliphatic chains of the FA remain bound within the hydrophobic cavity and that the barrier to dissociation reflects predominantly the cleavage of the nonpolar intermolecular interactions. In contrast, the E_a values determined for the *slow* components do not vary in a simple fashion with the length of the aliphatic chain. A possible explanation for this observation and the larger E_a values, compared to those of the $(\text{Lg} + \text{FA})_f^{7-}$ ions, is that the ligand carboxylic group stabilizes the $(\text{Lg} + \text{FA})_s^{7-}$ ions through its participation in H-bonds. As described below, the H-bond interactions are sensitive to the length of the aliphatic chain.

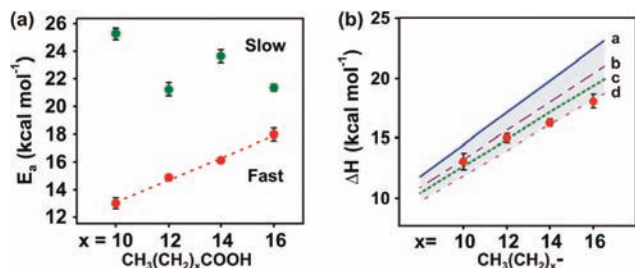


Figure 2. (a) Plot of activation energies (E_a) versus x for the dissociation of the $(\text{Lg} + \text{FA})_f^{7-}$ (red circles) and $(\text{Lg} + \text{FA})_s^{7-}$ ions (green circles). The dashed line corresponds to linear least-squares fit of the E_a values determined for the $(\text{Lg} + \text{FA})_f^{7-}$ ions. (b) Plot of the calculated solvation enthalpy (ΔH) of the aliphatic chain, $\text{CH}_3(\text{CH}_2)_x-$, versus x in (a) hexane, (b) benzene, (c) cyclohexane, (d) butanol. The E_a values for $(\text{Lg} + \text{FA})_f^{7-}$ (red circles) are shown for comparison.

The A -factors determined for the $(\text{Lg} + \text{FA})_f^{7-}$ ions translate to negative ΔS^\ddagger values, ranging from -22 to -9 cal mol⁻¹ K⁻¹, and indicate a loss of entropy in going from the reactant to the dissociative transition state (TS). The cleavage of the stabilizing intermolecular interactions is expected to be entropically favorable, and in fact, the ΔS^\ddagger values do become less negative as the length of the aliphatic chain increases. The negative ΔS^\ddagger values, therefore, imply a loss of Lg configurational entropy in the TS . This finding is consistent with the solution NMR results.⁵ However, as described below, the origin of these effects are likely different. In contrast, the loss of ligand from the $(\text{Lg} + \text{FA})_s^{7-}$ ions is an entropically neutral or somewhat favorable process. The larger ΔS^\ddagger values determined for the $(\text{Lg} + \text{FA})_s^{7-}$ ions are consistent with H-bonds stabilizing the complex and the substantial gain in entropy expected upon their dissociation.^{1e,9}

Molecular dynamics (MD) simulations performed on the $(\text{Lg} + \text{PA})$ complex at the -7 charge state and 25 °C suggest possible

structures for the $(\text{Lg} + \text{FA})_f^{7-}$ and $(\text{Lg} + \text{FA})_s^{7-}$ ions. Depending on the charge configuration, the $(\text{Lg} + \text{PA})_f^{7-}$ ion exists in one of two distinct structures, which differ primarily by the position of the EF loop. In the *open* structure, which is a possible candidate for the $(\text{Lg} + \text{PA})_f^{7-}$ ion, the EF loop is positioned away from the entrance to the cavity; the average distance between Asn88 on EF loop and Pro38 on AB loop (top of cavity) is ~21 Å (Figure S7a). The loss of PA from the *open* structure would require only the cleavage of the nonpolar intermolecular interactions. In the *closed* structure, a possible candidate for the $(\text{Lg} + \text{PA})_s^{7-}$ ion, the EF loop covers the entrance of the cavity, the average distance between Asn88 and Pro38 being ~15 Å, and the carboxylic group of PA participates in H-bonds with residues on the EF loop or residues located at the entrance (Figure S7b). The loss of ligand from the *closed* structure would require both the cleavage of the H-bonds and the nonpolar contacts and, as result, would proceed with an E_a larger than that of the *open* structure. The results of the MD simulations also suggest that the nature of intermolecular H-bonds vary between the $(\text{Lg} + \text{FA})_s^{7-}$ ions (Figure S8), which is consistent with the variations in the measured E_a values. Finally, MD simulations performed on the Lg^{7-} ion revealed that, independent of the charge configuration, the free protein adopts a single structure, which is characterized by the collapse of the hydrophobic cavity (Figure S9). Contraction of the cavity would be expected to result in a loss of protein configurational entropy, consistent with the observation of negative ΔS^\ddagger values.

In summary, the results of time-resolved thermal dissociation kinetic measurements and molecular modeling performed on a series of gaseous $(\text{Lg} + \text{FA})_f^{7-}$ ions provide evidence that the nonpolar intermolecular interactions implicated in the hydrophobic protein–ligand interactions are preserved in the gas phase. Furthermore, the strengths of these interactions have been quantified for the first time. The results of this work highlight the potential of gas phase studies for probing the nature of hydrophobic protein–ligand binding in solution.

Acknowledgment. The authors are grateful for financial support provided by the Natural Sciences and Engineering Research Council of Canada and the Alberta Ingenuity Centre for Carbohydrate Science.

Supporting Information Available: Experimental and computational methods, mass spectra, ion mobility data, structures from MD simulations. This material is available free of charge via the Internet at <http://pubs.acs.org>.

References

- (1) Wytenbach, T.; Bowers, M. T. *Annu. Rev. Phys. Chem.* **2007**, *58*, 511–533.
- (2) Rostom, A. A.; Tame, J. R. H.; Ladbury, J. E.; Robinson, C. V. *J. Mol. Biol.* **2000**, *296*, 269–279.
- (3) Kitova, E. N.; Bundle, D. R.; Klassen, J. S. *Angew. Chem., Int. Ed.* **2004**, *43*, 4183–4186.
- (4) Sun, J. X.; Kitova, E. N.; Klassen, J. S. *Anal. Chem.* **2007**, *79*, 417–425.
- (5) Kitova, E. N.; Seo, M.; Roy, P.-N.; Klassen, J. S. *J. Am. Chem. Soc.* **2008**, *130*, 1214–1226.
- (6) Wu, S.-Y.; Perez, M. D.; Puyol, P.; Sawyer, L. *J. Biol. Chem.* **1999**, *274*, 170–174.
- (7) (a) Kontopidis, G.; Holt, C.; Sawyer, L. *J. Dairy Sci.* **2004**, *87*, 785–796. (b) Qin, B. Y.; Bewley, M. C.; Creamer, L. K.; Baker, H. M.; Baker, E. N.; Jameson, G. B. *Biochemistry* **1998**, *37*, 14014–14023.
- (8) Qvist, J.; Davidovic, M.; Hamelberg, D.; Halle, B. *Proc. Natl. Acad. Sci. U.S.A.* **2008**, *105*, 6296–6301.
- (9) Konuma, T.; Sakurai, K.; Goto, Y. *J. Mol. Biol.* **2007**, *368*, 209–218.
- (10) (a) Dunbar, R. C.; McMahon, T. B. *Science* **1998**, *279*, 194–197. (b) Price, W. D.; Schnier, P. D.; Jockusch, R. A.; Strittmatter, E. R.; Williams, E. R. *J. Am. Chem. Soc.* **1996**, *118*, 10640–10644.
- (11) Fuchs, R.; Stephenson, W. K. *Can. J. Chem.* **1985**, *63*, 349.
- (12) Abraham, M. H. *J. Am. Chem. Soc.* **1982**, *104*, 2085–2094.
- (13) Kitova, E. N.; Bundle, D. R.; Klassen, J. S. *J. Am. Chem. Soc.* **2002**, *124*, 5902–5913.

JA9060454